

BARBARA BIAŁECKA¹, ZDZISŁAW ADAMCZYK², MAGDALENA CEMPA³

Synthesis of pitiglianoite and tobermorite from fly ash originating from lignite combustion

Introduction

Coal fly ash (CFA) separated from the flue gas stream constitutes a huge amount of waste generated worldwide. Due to environmental problems, many directions of their rational use have been developed, although the largest numbers are directed towards the cement industry and to the production of concrete (Ahmaruzzaman 2010). Various attempts to convert coal fly ash (CFA) into sorption materials, mainly synthetic zeolites, have been conducted successfully (Molina and Poole 2004; Moriyama et al. 2005; Bukhari et al. 2015; Lee et al. 2017; Belviso 2018).

Synthetic zeolites from CFB are usually obtained in the hydrothermal process (Adamczyk and Białecka 2005; Franus 2010; Musyoka et al. 2012; Deng et al. 2016), the alkaline fusion-assisted hydrothermal process (Musyoka et al. 2012; Wdowin et al. 2014; Kunecki et al. 2017), and the salt-thermal production process (Park et al. 2000). The hydrothermal process is discussed in more detail below.

✉ Corresponding Author: Magdalena Cempa; e-mail: mcempa@gig.eu

¹ Central Mining Institute, Katowice, Poland; ORCID iD: 0000-0002-6002-5475; e-mail: bbialecka@gig.eu

² Silesian University of Technology, Gliwice, Poland; ORCID iD: 0000-0002-5925-4676;
e-mail: zdzislaw.adamczyk@polsl.pl

³ Central Mining Institute, Katowice, Poland; ORCID iD: 0000-0002-4779-1263; e-mail: mcempa@gig.eu



© 2019. The Author(s). This is an open-access article distributed under the terms of the Creative Commons Attribution-ShareAlike International License (CC BY-SA 4.0, <http://creativecommons.org/licenses/by-sa/4.0/>), which permits use, distribution, and reproduction in any medium, provided that the Article is properly cited.

CFA is subject to the direct effect of alkaline solutions (NaOH, KOH) under specified conditions (solution concentration, solution/fly ash ratio, temperature, pressure and time) to obtain synthetic zeolite materials (Querol et al. 2002). Ash is often given to the pre-treatment process before the fundamental synthesis i.e. the action of acids, seeding, ageing (Zhao et al. 1997; Panitchakarn et al. 2014). Hydrothermal conversion can be assisted by using microwave or ultrasound waves (Bukhari et al. 2015). The composition of ash is important in the synthesis of zeolites on the basis CFA, especially the $\text{SiO}_2/\text{Al}_2\text{O}_3$ ratio and content of glass (Tanaka and Fujii 2009; Zhang et al. 2017). Various additives to the reaction solution are used to adjust the ratio of aluminum to silicon e.g. NaAl_2O_3 as aluminum source or e.g. colloidal silica as silicon source (Zhao et al. 1997; Li and Yo 2010). Other additives used in the synthesis include: NaCl, KCl, and a nucleating agent (Zhao et al. 1997; Li, Yo 2010). The synthesis is usually carried out at a temperature of 50 to 180°C (Zhao et al. 1997; Kotova et al. 2016). Zeolite products can also be obtained by running the process at room temperature, but increasing the process temperature significantly extends the process time, even up to several months (Franus 2010). The various types of zeolite materials depending on the used synthesis conditions are obtained in the hydrothermal process e.g.: Na-P1 zeolite, X-type zeolite, A-type zeolite, Y-type zeolite, hydroxy-cancrinite, herschelite, pitiglianoite (Querol et al. 2001; Bukhari et al. 2015; Lee et al. 2017; Belviso 2018).

In this paper, an attempt was made to convert fly ash from lignite combustion from one of the Polish power plants, using alkaline hydrothermal synthesis.

1. Materials and methods

The synthesis of pitiglianoite was carried out on the basis of fly ash derived from the combustion of lignite at the Bełchatów Power Plant.

Fly ash was subjected to hydrothermal synthesis in an autoclave. The synthesis was carried out with aqueous solution of NaOH and KOH at the temperature of 170°C.

The identification of minerals in the raw ash sample as well as in the material after the synthesis was performed using microscopic observations (Zeiss Axioskop microscope), scanning electron microscopy with the possibility of determining the chemical composition in the micro-area (SEM SU3500 microscope by Hitachi, cooperating with an X-ray spectrometer with energy dispersion EDS UltraDry from Thermo Scientific NORAN System 7) and X-ray diffraction (AERIS 1 diffractometer by PANalytical, $\text{CuK}\alpha$ radiation). The chemical composition of raw ash and material after synthesis was determined using fluorescence X-ray spectrometry (PANalytical Epsilon 1 spectrometer).

For the fly ash sample and products after synthesis, a thermal analysis was performed using the SDT Q600 TA Instruments analyzed under the following conditions: sample weight: approx. 20 mg, temperature range: 22–1000°C, temperature increase: 10°C/min, atmosphere: air.

2. Results and discussion

The chemical composition of the fly ash under investigation, similarly as it has already been demonstrated in another paper (Adamczyk et al. 2018), was dominated by SiO₂ and CaO, together constituting over 64% mas. The Al₂O₃ content was over 19% mas., while Fe₂O₃ about 5% mas., and SO₃ above 3% mas. The participation of other chemical components was significantly lower (Table 1).

The presence of quartz, gehlenite, mullite, hematite, feldspar, lime, anhydrite, occasionally grains of ZnO phase and pyrrhotite, glass and grains of unburned fuel was found in the mineral composition of the fly ash under investigation, as a result of microscopic observations, scanning electron microscopy and X-ray diffraction (Adamczyk et al. 2018). This confirms the findings of studies carried out previously. Grains were irregular or had spherical shapes and formed polyphasic aggregates, whereas single-phase grains were less frequent (Figs. 1–2).

The presence of pitiglianoite, tobermorite and gehlenite was found in the material after the hydrothermal synthesis of fly ash from the combustion of lignite. Characteristic reflections originating from these phases were found on the diffractogram of the tested material

Table 1. Chemical composition of fly ash from lignite combustion and material after synthesis (% mas.)

Tabela 1. Skład chemiczny popiołu lotnego pochodzącego ze spalania węgla brunatnego oraz materiału po syntezie (% mas.)

Chemical composition	Initial sample*	Initial sample	Material after synthesis
SiO ₂	32.85	40.19	30.73
TiO ₂	1.48	1.23	1.04
Al ₂ O ₃	18.45	19.77	15.96
Fe ₂ O ₃	7.04	5.51	4.94
MnO	0.07	0.07	0.05
MgO	1.37	1.39	0.70
CaO	31.60	24.13	20.92
Na ₂ O	0.13	0.27	8.31
K ₂ O	0.14	0.15	7.26
SO ₃	6.81	3.29	2.94
Cl	0.04		0.04
LOI		3.31	6.91
Total	100.00	99.31	99.80

* Adamczyk et al. 2018.

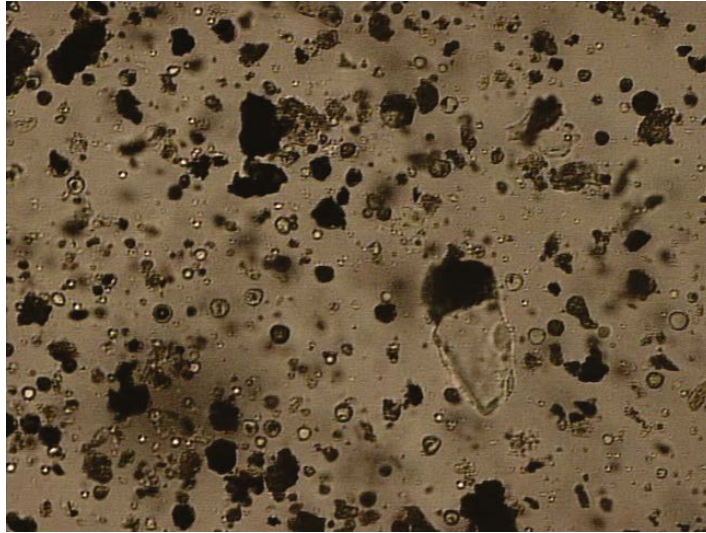


Fig. 1. Microscopic image of glass grains, quartz and unburned coal in fly ash from Belchatów Power Station, transmitted light, one nicol, 400× magnification

Rys. 1. Obraz mikroskopowy ziaren szkliva, kwarcu i nieprzealonego węgla w popiele lotnym z Elektrowni Belchatów, światło przechodzące, jeden nikol, powiększenie 400×

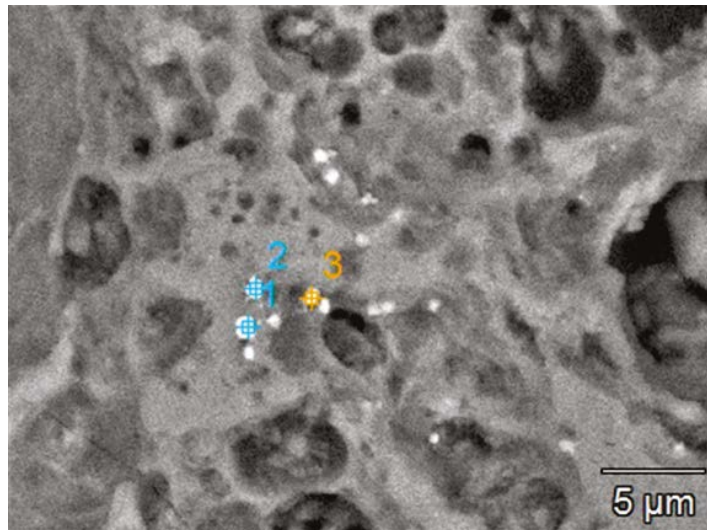


Fig. 2. SEM image of pyrrhotite grains in highly porous glass in fly ash from Belchatów Power Station

Rys. 2. Obraz SEM ziaren pirytynu w silnie porowatym szkliwie w popiele lotnym z Elektrowni Belchatów

(Fig. 4). It is noteworthy that there are no reflections from other phases present in the sample of raw fly ash (quartz, feldspar, hematite, lime, anhydrite), with the exception of gehlenite. Microscopic observations revealed that after synthesis an unburned organic substance is also formed in the products (Figs. 5–6), and the newly formed phases (pitiglianoite and tobermorite) agglutinate the relict ash grains (Figs. 7–8).

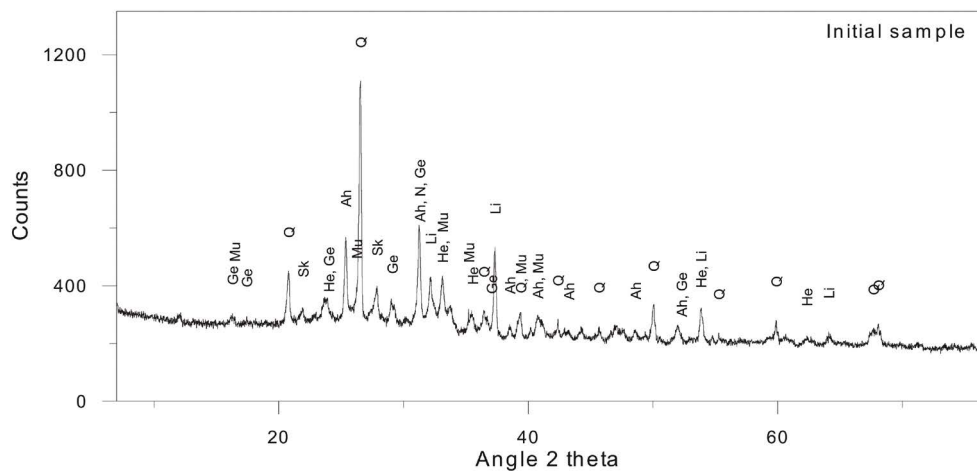


Fig. 3. X – ray diffraction pattern of fly ash from Belchatów Power Plant
Q – quartz, Sk – feldspar, He – hematite, Li – lime, Ah – anhydrite, Ge – gehlenite

Rys. 3. Widmo XRD popiołu lotnego z Elektrowni Belchatów
Q – kwarc, Sk – skałen, He – hematyt, Li – lime, Ah – anhydryt, Ge – gehlenit

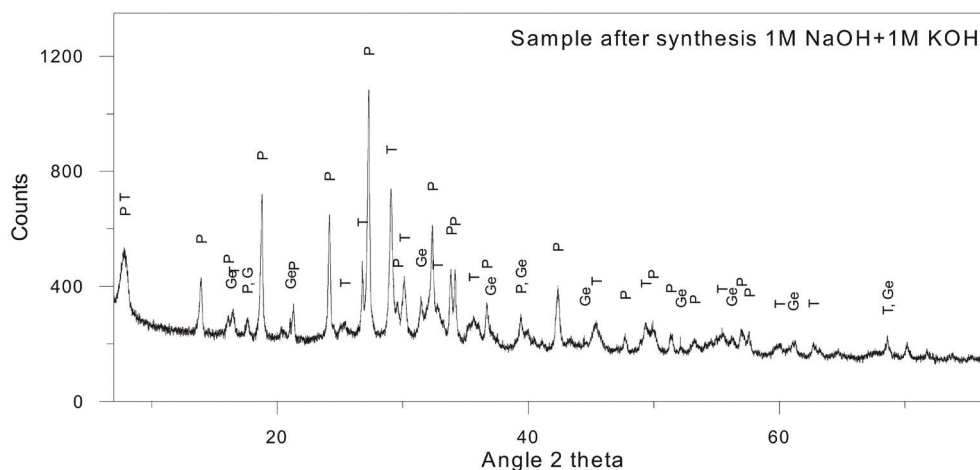


Fig. 4. X – ray diffraction pattern of fly ash from Belchatów Power Plant after synthesis
Ge – gehlenite, P – pitiglianoite, T – tobermorite

Rys. 4. Widmo XRD popiołu lotnego z Elektrowni Belchatów po syntezie
Ge – gehlenit, P – pitiglianoit, T – tobermoryt

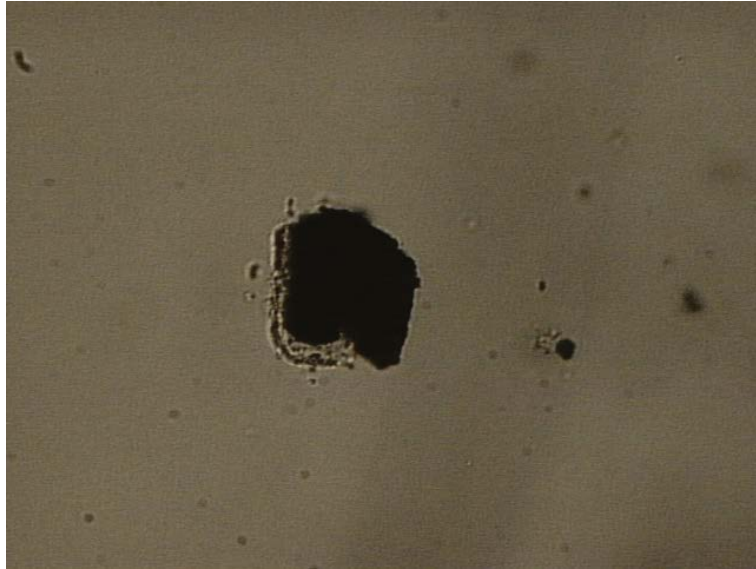


Fig. 5. Microscopic image of hydrothermal synthesis products agglutinating coal grain, transmitted light, one nicol, 400× magnification

Rys. 5. Obraz mikroskopowy produktów po syntezie hydrotermalnej oblepiających ziarno węgla, światło przechodzące, jeden nikol, powiększenie 400×

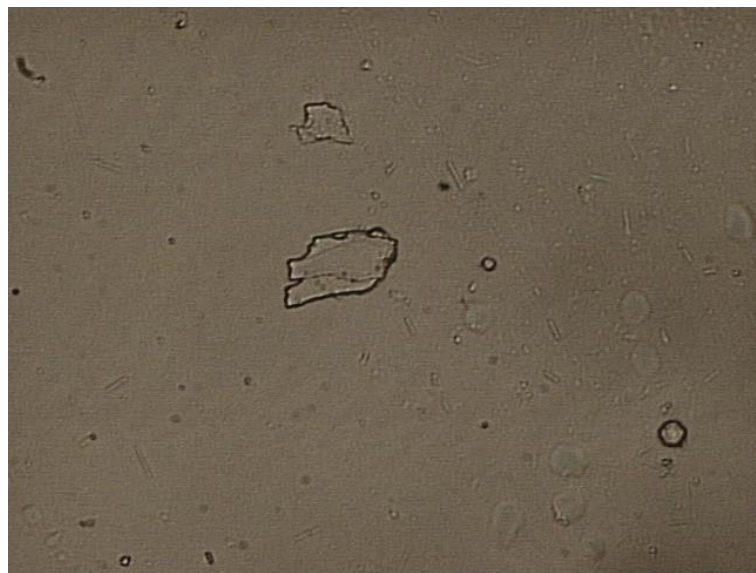


Fig. 6. Microscope image of hydrothermal synthesis products, transmitted light, one nicol, 400× magnification

Rys. 6. Obraz mikroskopowy produktów po syntezie hydrotermalnej, światło przechodzące, jeden nikol, powiększenie 400×

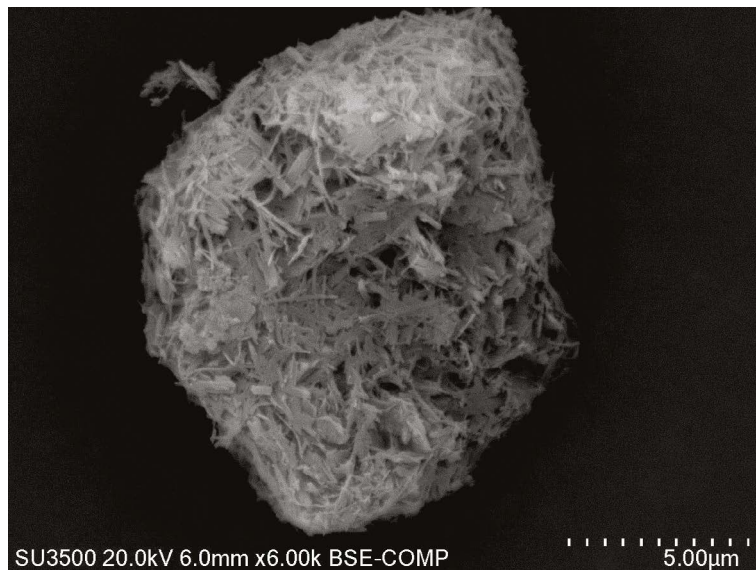


Fig. 7. SEM image of tobermorite rods and pitiglianoite bars, 6000× magnification

Rys. 7. Obraz SEM przecików tobermorytu i słupków pitiglianoitu, powiększenie 6000×

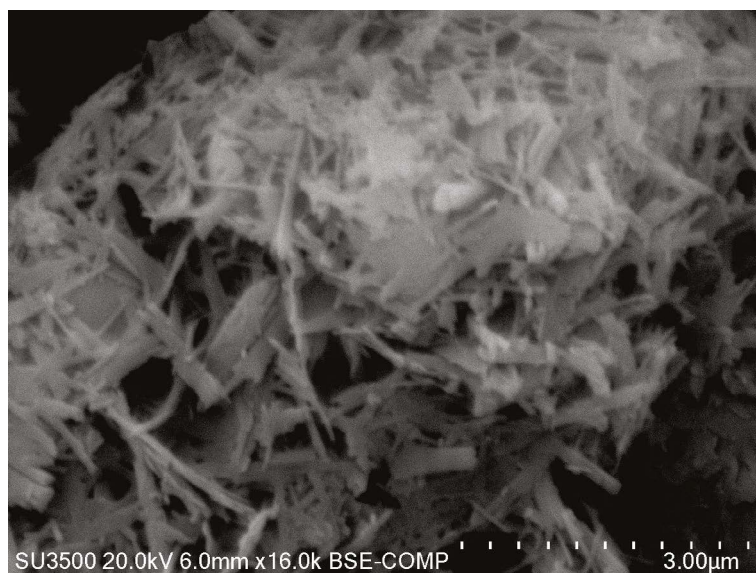


Fig. 8. SEM image of tobermorite rods and pitiglianoite bars, 16 000× magnification

Rys. 8. Obraz SEM przecików tobermorytu i słupków pitiglianoitu, powiększenie 16 000×

Detailed studies in scanning electron microscopy confirm the mineral composition of products after synthesis, because tobermorite crystallizes in the form of characteristic rods, while pitiglianoite in formed bars. It is noteworthy that both phases usually overwhelm each other, and gehlenite grains are covered with both tobermorite and pitiglianoite. This is also proven by the chemical composition in the micro-areas (Table 2).

There was no chemical composition in any of the micro areas that would correspond to stoichiometric tobermorite, pitiglianoite or gehlenite.

Only a few measuring points are in the pitiglianoite field in the diagram in the SiO_2 – Al_2O_3 system, where the fields of theoretical differentiation of the content of these components for pitiglianoite, tobermorite and gehlenite are schematically marked (Fig. 9). Most of the studied grains are arranged between pitiglianoite and tobermorite fields, with a higher concentration of points near the pitiglianoite field.

A similar diagram was prepared for the Al_2O_3 – CaO system (with schematically marked fields of theoretical variation in the content of these components for pitiglianoite, tobermorite and gehlenite). Similarly to the SiO_2 – Al_2O_3 system, the measurement points become more concentrated closer to the pitiglianoite field (Fig. 10), they are arranged between pitiglianoite and tobermorite fields.

The sum of CaO and MgO and sum of Na_2O and K_2O in the studied grains is very interesting, indicating a high correlation ($R^2 = 0.88$), which reveals that together with the increase in the sum of CaO and MgO participation, the sum of Na_2O and K_2O decreases (Fig. 11).

Table 2. Basic statistics of chemical composition of grains in products after synthesis (% mas.)

Tabela 2. Podstawowe statystyki składu chemicznego ziaren w produktach po syntezie (% mas.)

		SiO_2	TiO_2	Al_2O_3	Fe_2O_3	MgO	CaO	Na_2O	K_2O	SO_3	Number of grains
A	Min.	33.57	0.00	12.68	0.55	0.12	3.78	3.52	4.47	1.31	25
	Max.	47.37	1.44	26.73	3.46	2.31	22.25	20.59	9.96	6.82	
	S	38.17	0.31	21.96	1.76	0.80	12.45	12.17	7.56	4.83	
	SD	3.18	0.42	3.25	0.91	0.45	3.97	3.59	1.43	1.24	
	V (%)	8.33	137.99	14.78	51.77	56.99	31.91	29.47	18.91	25.63	
B	Min.	33.59	0.00	13.86	0.00	0.00	4.30	6.05	5.39	3.79	41
	Max.	44.21	1.55	27.39	4.71	1.36	21.61	21.11	11.09	7.47	
	S	38.14	0.19	22.73	0.63	0.18	11.01	13.08	8.32	5.71	
	SD	2.52	0.44	3.35	1.23	0.38	4.97	3.63	1.39	0.87	
	V (%)	6.61	228.47	14.74	193.40	213.99	45.13	27.76	16.73	15.22	

Min. – minimum content, Max. – maximum content, S – average, SD – standard deviation of mean S, V – coefficient of variation.

Due to the chemical composition, two populations were distinguished among the examined grains – grains containing MgO and Fe₂O₃ (population A, Table 1) as well as grains containing Fe₂O₃ or MgO or containing none of these components (population B, Table 1). Basic statistical parameters for the majority of chemical components in both populations reveal little variation in them, which is supported by similar values of both the arithmetic mean and the coefficient of variation (Table 1). However, the values of the coefficient of variation for the content of TiO₂, Fe₂O₃ and MgO, which for grains containing MgO and Fe₂O₃ are for TiO₂ approx. 138%, for Fe₂O₃ – approx. 52%, and for MgO – approx. 57%.

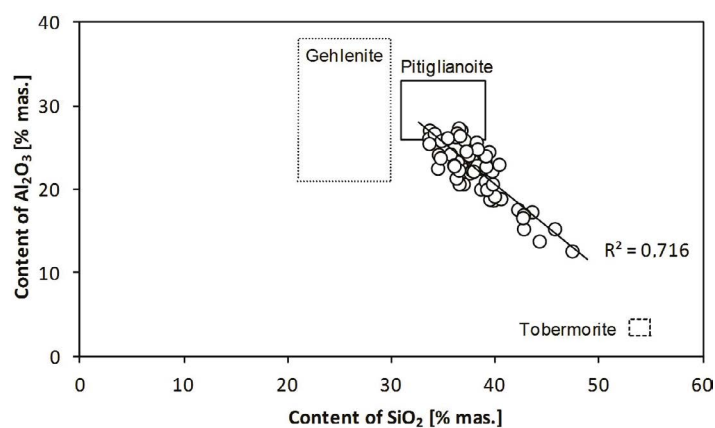


Fig. 9. Participation of SiO₂ and Al₂O₃ in the studied grains against the background of the theoretical differentiation of the content of these components in tobermorite, pitiglianoite and gehlenite

Rys. 9. Udział SiO₂ i Al₂O₃ w badanych ziarnach na tle teoretycznego zróżnicowania zawartości tych składników w tobermorycie, pitiglianoicie i gehlenicie

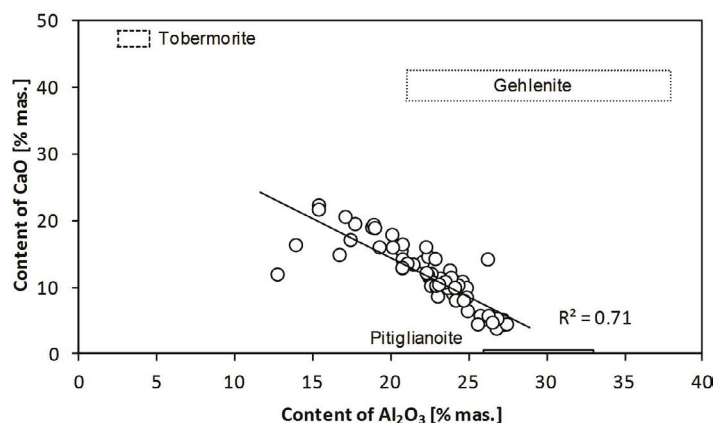


Fig. 10. Participation of Al₂O₃ and CaO in the studied grains against the background of the theoretical differentiation of the content of these components in the tobermorite, pitiglianoite and gehlenite

Rys. 10. Udział Al₂O₃ i CaO w badanych ziarnach na tle teoretycznego zróżnicowania zawartości tych składników w tobermorycie, pitiglianoicie i gehlenicie

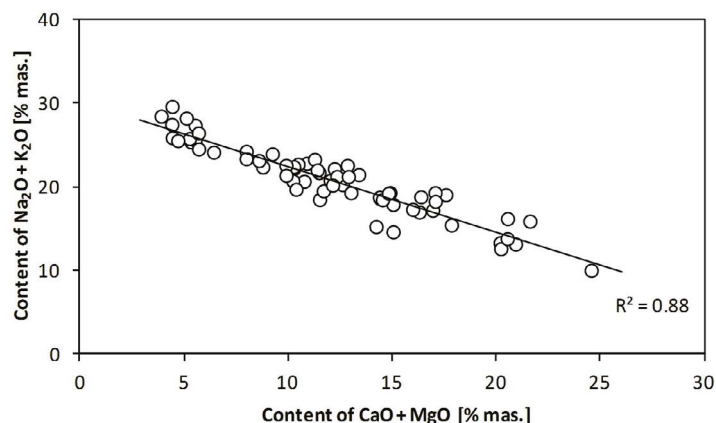


Fig. 11. Participation of the sum of CaO and MgO and the sum of Na₂O and K₂O in the examined grains

Rys. 11. Udział sumy CaO i MgO oraz sumy Na₂O i K₂O w badanych ziarnach

For grains containing Fe₂O₃ or MgO, or not containing both of these components, the coefficient of variation for TiO₂, Fe₂O₃ and MgO content are respectively ca. 228%, ca. 193% and ca. 214%. This clearly indicates a significant differentiation of these chemical components in the studied grains, and therefore their polymineral nature.

In a population of grains containing MgO and Fe₂O₃, some relationships have been noticed that are characteristic of it, compared to grains containing Fe₂O₃ or MgO or not containing any of these components. They are characterized by the distinction of two groups of grains, for which the division limit is the Fe₂O₃ content, amounting to 2%mas., for which it was found that (Figs. 12–13):

- ◆ there is a high positive linear correlation between MgO and Fe₂O₃ ($R_2 = 0.71$) for grains < 2%mas. of Fe₂O₃, while CaO and Fe₂O₃ ($R^2 = 0.78$),
- ◆ there is a high negative linear correlation between MgO and Fe₂O₃ ($R_2 = 0.79$) for grains > 2%mas. of Fe₂O₃, while CaO and Fe₂O₃ ($R^2 = 0.78$).

There was also a high linear correlation between CaO and MgO in grains where MgO was found ($R^2 = 0.80$) (Figure 14).

As is well known, both pitiglianoite – $K_2Na_6Si_6Al_6O_{24}(SO_4) \cdot 2H_2O$, and tobermorite – $Ca_5Si_6O_{16}(OH)_2 \cdot 4H_2O$, do not contain magnesium or iron in their chemical composition, only in trace amounts (Mitsuda and Taylor 1978; Leoni et al. 1979; Livingstone 1988; Anthony et al. 1990; Merlino et al. 1991; Henmi and Kusachi 1992; Jackson et al. 2017). It can therefore be concluded that both of these components (MgO and Fe₂O₃) are part of the gehlenite, forming adhesions with pitiglianoite and tobermorite. This is also supported by the increase in the proportion of CaO together with the increase in MgO content in grains containing MgO. These considerations may prove that apart from gehlenite – $Ca_2Al(Al,Si)O_7$, the presence of akermanite – $Ca_2MgSi_2O_7$, and even melilite – $(Ca,Na)_2(Al,Mg,Fe)(Si,Al)_2O_7$, phases belonging to the melilite group, is possible in the sample after synthesis.

SO₃ is an important chemical component of the analyzed grains indicating the presence of pitiglianoite. The content of this component does not exceed 7%mas. in grains containing Fe₂O₃ and MgO, in grains containing Fe₂O₃ or MgO, or in the absence of both components, the SO₃ content approaches 7.5%mas. (Table 2). This is justified for obvious reasons, because the higher proportion of SO₃ indicates a higher participation of pitiglianoite, which both Fe₂O₃, as well as MgO are not part of. Theoretically, the SO₃ content in pitiglianoite can range from 5.60 to 7.60% mas. (Merlino et al. 1991; Bonaccorsi and Orlandi 1996; Pekov et al. 2011).

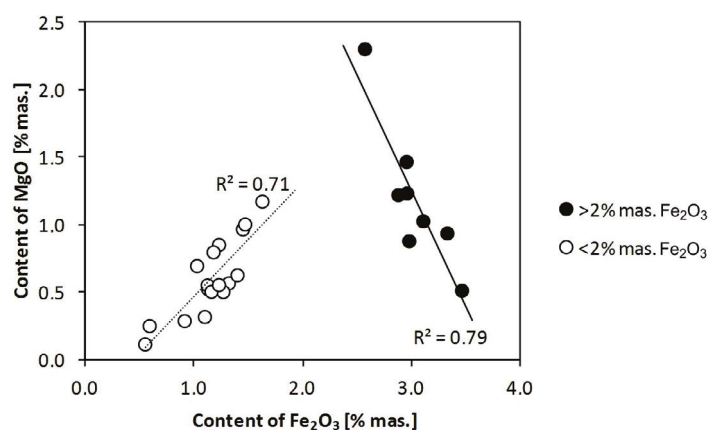


Fig. 12. Variability of Fe₂O₃ and MgO participation in the analysed grains (description in the text)

Rys. 12. Zmienność udziału Fe₂O₃ i MgO w badanych ziarnach (opis w tekście)

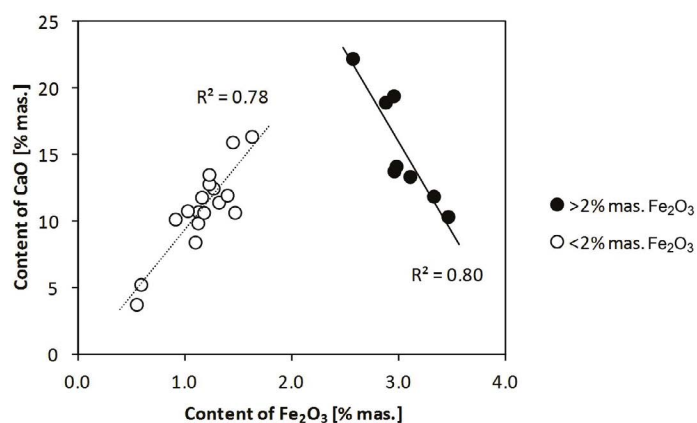


Fig. 13. Variability of Fe₂O₃ and CaO participation in the analysed grains (description in the text)

Rys. 13. Zmienność udziału Fe₂O₃ i CaO w badanych ziarnach (opis w tekście)

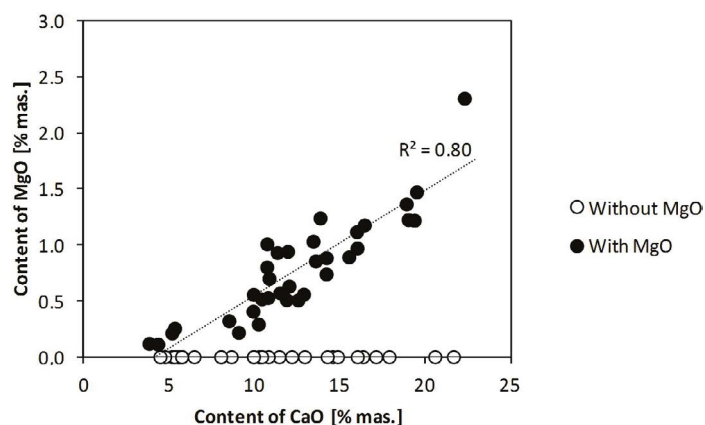


Fig. 14. Variability of CaO and MgO participation in the analyzed grains

Rys. 14. Zmienność udziału CaO i MgO w badanych ziarnach

Therefore, the participation of pitiglianoite could be varied in the studied grains, hence calculations of the share of the main phases (pitiglianoite, tobermorite and melilites) in them, taking their chemical formulas into account. These calculations clearly indicate (Table 3) that the contribution of pitiglianoite was higher in grains containing Fe_2O_3 or MgO or in the absence of both components (approx. 71% mas.), than in grains where Fe_2O_3 and MgO were found (approx. 61% mas.).

Table 3. Basic statistics on the proportion of phases in the examined product grains after synthesis (% mas.)

Tabela 3. Podstawowe statystyki udziału faz w badanych ziarnach produktów po syntezie (% mas.)

		Pitiglianoite	Tobermorite	Melilite	Number of grains
A	Min.	16.80	0.00	3.71	25
	Max.	83.43	28.74	81.50	
	S	61.07	10.44	28.49	
	SD	14.88	9.07	16.80	
	V (%)	24.36	86.91	58.97	
B	Min.	40.72	0.00	2.47	41
	Max.	95.60	46.16	42.82	
	S	70.71	10.98	18.30	
	SD	12.29	11.41	9.80	
	V (%)	17.38	103.92	53.53	

Min. – minimum content, Max. – maximum content, S – average, SD – standard deviation of mean S, V – coefficient of variation.

The results of these conversions were presented in the pitiglianoite-tobermorite-melilites system (Fig. 14). The majority of projection points concentrate in the vicinity of pitiglianoite, which clearly indicates a high proportion of this component in the analyzed grains. These points are dominated by grains containing Fe_2O_3 or MgO or the absence of both components. Therefore, it should be concluded that tobermorite crystallized on gehlenite first and on pitiglianoite later.

The thermal curve of fly ash mass loss exhibits a weight loss of 3.35% at a temperature of 1000°C , which is mainly related to the oxidation of unburned fuel and corresponds with the share of LOI (Fig. 16, Table 1). The weight loss is mainly observed in the temperature range from $400\text{--}660^\circ\text{C}$.

After the synthesis, the material shows a weight loss of 12.48% at a temperature of 1000°C , with a substantial drop in the temperature range from $22\text{--}500^\circ\text{C}$.

The characteristics of the thermal curve of mass loss of both pitiglianoite and tobermorite, in the temperature range from $22\text{--}500^\circ\text{C}$, is very similar because in both phases there is a decrease in mass associated with their dehydration and the possible degassing of pitiglianoite (Farmer et al. 1966; Huang et al. 2002; Maeshima et al. 2003; Galvankova et al. 2016). As research shows (Bonaccorsi et al. 2007), there is still a small amount of water in

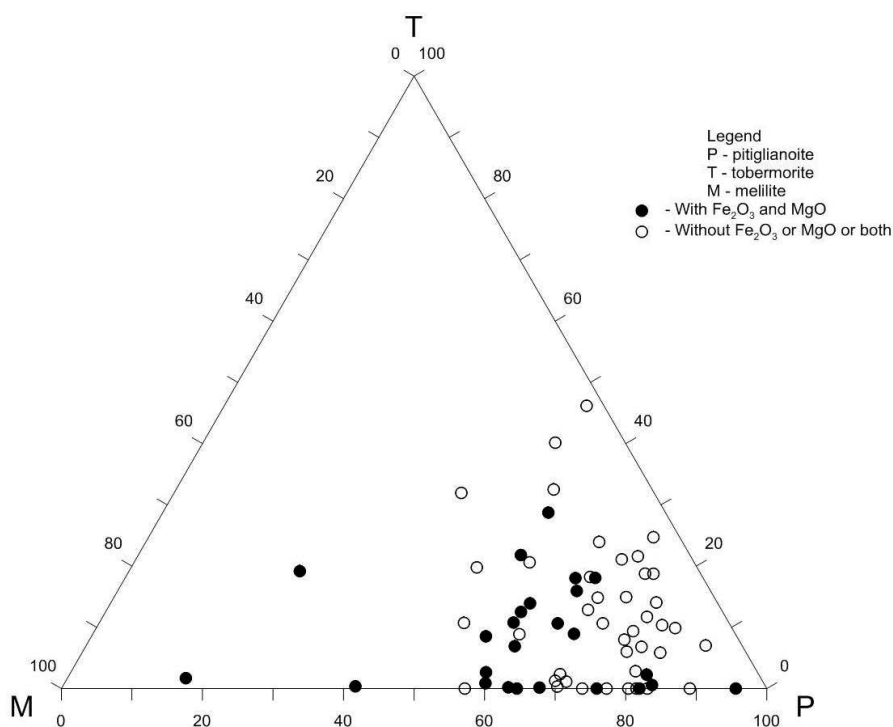


Fig. 15. Projection of analysed grains in the pitiglianoite-tobermorite-melilites system (phase proportions in % mas.)

Rys. 15. Projekcja badanych ziaren w układzie pitiglianoit-tobermoryt-melility (udziały faz w % mas.)

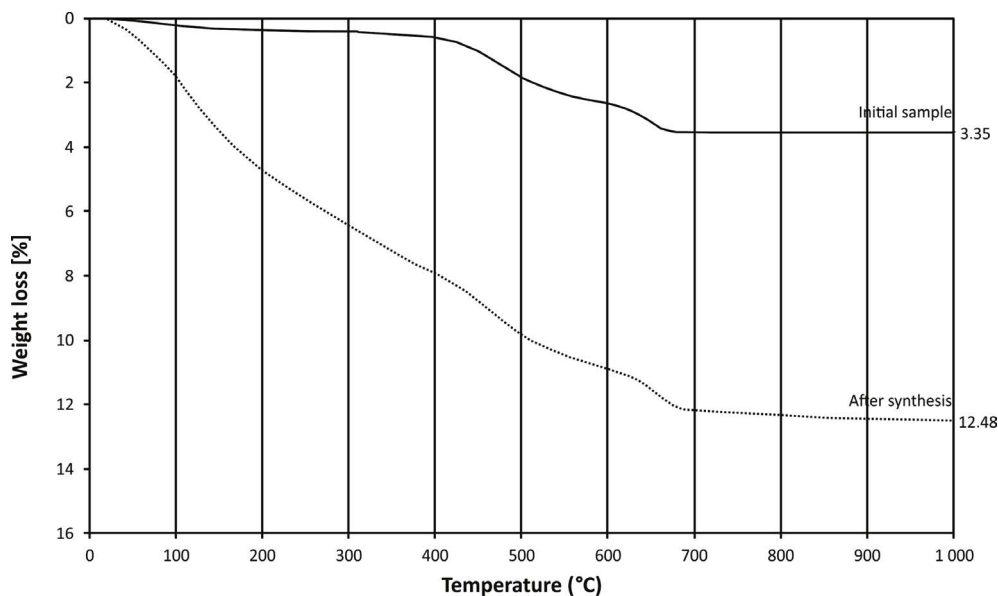


Fig. 16. Mass loss curves for a raw fly ash sample and a product after synthesis

Rys. 16. Krzywe ubytku masy dla surowej próbki popiołu lotnego i produktu po syntezie

pitiglianoite at a temperature above 400°C, and pitiglianoite becomes anhydrous at a temperature of about 500°C (Bonaccorosi et al. 2007; Chukanov et al. 2011). The course of the thermal curves of the weight loss of both the fly ash initial sample and the synthesis products in the temperature range from 400–690°C is similar (Fig. 16). However, the weight loss is slightly larger on the curve of the synthesis products (4.22%) compared to the initial sample (2.94%). This clearly indicates that the mass decrease in this temperature range in synthesis products is related not only to the presence of unburned fuel in both samples, but also to the last stage of pitiglianoite dehydration.

It can therefore be assumed that the total loss of mass of new phases (pitiglianoite and tobermorite) in products after synthesis (mellite does not show a weight loss), after taking the weight loss related to the presence of unburned fuel into account, is 8.90%. Assuming the theoretical water content in pitiglianoite (3.39% mas.) and tobermorite (12.82% mas.), the shares of these two phases in products after synthesis are 42% mas. and 58% mas., respectively.

Conclusion

The primary phases in the fly ash from the combustion of lignite were: quartz, gehlenite, mullite, hematite, feldspar, lime, anhydrite, occasionally grains of ZnO phase and pyrrhotite, glass and unburned fuel grains.

As a result of hydrothermal synthesis carried out in an autoclave at 170°C, in a water solution of NaOH and KOH, a material containing new phases – pitiglianoite and tobermorite, was obtained. Among the primary ash constituents, only gehlenite with an unburned organic substance, on which tobermorite with pitiglianoite crystallized, was present.

Pitiglianoite crystallized in the form of characteristic bars, while tobermorite formed rods, and both phases usually overwhelm each other, clinging to the original, relic grains of fly ash (gehlenite and unburned organic substance).

As a result of detailed testing of products after synthesis, it was found that among the tested grains:

- ◆ two populations can be distinguished – grains containing MgO and Fe₂O₃ as well as grains containing Fe₂O₃ or MgO or containing none of these components,
- ◆ the main quantitative component was pitiglianoite,
- ◆ pitiglianoite was present in larger amounts in grains containing Fe₂O₃ or MgO or in the absence of both components than in grains in which Fe₂O₃ and MgO were found.

In post-synthesis products, the contribution of components were as follows: pitiglianoite – 39.5% mas., tobermorite – 54% mas., gehlenite – 3% mas. and organic substance – 3.5% mas.

The paper has been prepared in the frames of the: “Innovative Management of COAL BY-PRODUCTS leading also to CO₂ emissions reduction” project funded by the Ministry of Science and Higher Education (Republic of Poland) and the European Commission under the Research Fund for Coal and Steel (RFCS-2016).

REFERENCES

- Adamczyk, Z. and Białecka, B. 2005. Hydrothermal Synthesis of Zeolites from Polish Coal Fly Ash. *Polish Journal of Environmental Studies* 14(6), pp. 713–719.
- Adamczyk et al. 2018 – Adamczyk, Z., Białecka, B., Cempa, M., Majka, G. and Polańska, A. 2018. Hydrothermal activation of fly ash from brown coal combustion [In:] Conference proceedings. Vol. 18. Science and technologies in geology, exploration and mining. Iss. 1.4. Mineral processing, oil and gas exploration. 18th International Multidisciplinary Scientific GeoConference. SGEM 2018. Albena, 2-8 July 2018. Sofia: STEF92 Technology Ltd., pp. 83–90.
- Ahmaruzzaman, M. 2010. A review on the utilization of fly Ash. *Progress in Energy and Combustion Science* 36(3), pp. 327–363.
- Anthony et al. 1990 – Anthony, J.W., Bideaux, R.A., Bladh, K.W. and Nichols, M.C. Eds. 1990. *Handbook of Mineralogy*. Tucson Arizona, USA: Mineral Data Pub.
- Belviso, C. 2018. State-of-the-art applications of fly ash from coal and biomass: A focus on zeolite synthesis processes and issues. *Progress in Energy and Combustion Science* 65, pp. 109–135.
- Bonaccorsi, E. and Orlandi, P. 1996. Second occurrence of pitiglianoite, a mineral of the cancrinite-group. *Atti Soc. Tosc. Sci. Nat., Mem., Serie A* 103, pp. 193–195.
- Bukhari et al. 2015 – Bukhari, S.S., Behin, J., Kazemian, H. and Rohani, S. 2015. Conversion of coal fly ash to zeolite utilizing microwave and ultrasound energies: A review. *Fuel* 140, pp. 250–266.

- Chukanov et al. 2011 – Chukanov, N.V., Pekov, I.V., Olysysh, L.V., Zubkova, N.V. and Vigasina, M.F. 2011. Crystal chemistry of cancrinite-group minerals with an AB-type framework: A review and new data. II. IR spectroscopy and its crystal-chemical implications. *The Canadian Mineralogist* 49, pp. 1151–1164.
- Deng et al. 2016 – Deng, L., Xu, Q. and Wua, H. 2016. Synthesis of zeolite-like material by hydrothermal and fusion methods using municipal solid waste fly ash. *Procedia Environmental Sciences* 31, pp. 662–667.
- Farmer et al. 1966 – Farmer, V.C., Jeevaratnam, J., Speakman, K. and Taylor, H.F.W. 1966. Thermal decomposition of 14 Å Tobermorite from Crestmore. *Symposium on Structure of Portland Cement Paste and Concrete, Spec. Rep.* 90, U.S. Highway Res. Board, Washington, pp. 291–299.
- Franus, W. 2010. Materiał zeolitowy typu X otrzymany z popiołu lotnego w wyniku syntezy hydrotermalnej i niskotemperaturowej. *Budownictwo i Architektura* 7, pp. 25–34.
- Galvankova et al. 2016 – Galvankova, L., Masilko, J., Solny, T. and Stepankova, E. 2016. Tobermorite synthesis under hydrothermal conditions. *Procedia Engineering* 151, pp. 100–107.
- Henmi, C. and Kusachi, I. 1992. Clinotobermorite, $\text{Ca}_5\text{Si}_6(\text{O},\text{OH})_{18} \cdot 5\text{H}_2\text{O}$, a new mineral from Fuka, Okayama Prefecture, Japan. *Mineralogical Magazine* 56, pp. 353–358.
- Huang et al. 2002 – Huang, X., Jiand, D. and Tan, S. 2002. Novel hydrothermal synthesis metod for tobermorite fibers and investigation on their thermal stability. *Materials Research Bulletin* 37, pp.1885–1892.
- Jackson et al. 2017 – Jackson, M.D., Mulcahy, S.R., Chen, H., Li, Y., Li, Q., Cappelletti, R. and Wenk, H.R. 2017. Phillipsite and Al-tobermorite mineral cements produced through low-temperature water-rock reactions in Roman marine concrete. *American Mineralogist* 102, pp. 1435–1450.
- Kotova et al. 2016 – Kotova, O.B., Shabalin, I.N., Shushkov, D.A. and Kocheva, L.S. 2016. Hydrothermal synthesis of zeolites from coal fly ash. *Advances in Applied Ceramics*, 115(3), pp.152–157.
- Kunecki et al. 2017 – Kunecki, P., Panek, R., Wdowin, M. and Franus, W. 2017. Synthesis of faujasite (FAU) and tschernichite (LTA) type zeolites as a potential direction of the development of lime Class C fly ash. *International Journal of Mineral Processing* 166, pp. 69–78.
- Lee, K.-M. and Jo, Y.-M. 2010. Synthesis of zeolite from waste fly ash for adsorption of CO_2 . *Journal of Material Cycles and Waste Management* 12(3), pp. 212–219.
- Lee et al. 2017 – Lee, Y.-R., Soe, J.T., Zhang, S., Ahn, J.-W., Park, M.B. and Ahn, W.-S. 2017. Synthesis of nanoporous materials via recycling coal fly ash and other solid wastes: A mini review. *Chemical Engineering Journal* 317, pp. 821–843.
- Leoni et al. 1979 – Leoni, L., Mellini, M., Merlino, S. and Orlandi, P. 1979. Cancrinite-like minerale: New data and crystal chemical consideration. *Rendiconti della Società Italiana di Mineralogia e Petrologia* 35(2), pp. 713–719.
- Livingstone A. 1988. Reyerite, tobermorite, calcian analcime and bytownite from amygdales in a Skye basalt. *Mineralogical Magazine* 52, pp. 711–713.
- Maeshima et al. 2003 – Maeshima, T., Noma, H., Sakiyama, M. and Mitsuda, T. 2003. Natural 1.1 and 1.4 nm tobermorites from Fuka, Okayama, Japan: Chemical analysis, cell dimensions, ^{29}Si NMR thermal behavior. *Cement and Concrete Research* 33, pp. 1515–1523.
- Merlino et al. 1991 – Merlino, S., Mellini, M., Bonaccorsi, E., Pasero, M., Leoni, L. and Orlandi, P. 1991. Pitiglianoite, a new feldspathoid from southern Tuscany, Italy: Chemical composition and crystal structure. *American Mineralogist* 76, pp. 2003–2008.
- Mitsuda, T. and Taylor, H.F. 1978. Normal and anomalous tobermorites. *Mineralogical Magazine* 42, pp. 229–235.
- Molina, A. and Poole, C. 2004. A comparative study using two methods to produce zeolites from fly ash. *Minerals Engineering* 17(2), pp. 167–173.
- Moriyama et al. 2005 – Moriyama, R., Takeda, S., Onozaki, M., Katayama, Y., Shiota, K., Fukuda, T., Sugihara, H. and Tani, Y. 2005. Large-scale synthesis of artificial zeolite from coal fly ash with a small charge of alkaline solution. *Fuel* 84(12–13), pp. 1455–1461.
- Musyoka et al. 2012 – Musyoka, N.M., Petrik, L. and Hums E. 2012. Synthesis of zeolite A, X and P from a South African coal fly ash. *Advanced Materials Research* 512–515, pp. 1757–1762.
- Panitchakarn et al. 2014 – Panitchakarn, P., Laosiripojana, N., Viriya-umpikul, N. and Pavasant, P. 2014. Synthesis of high-purity Na-A and Na-X zeolite from coal fly ash. *Journal of the Air & Waste Management Association* 64(5), pp. 586–596.

- Park et al. 2000 – Park, M., Choi, C.L., Lim, W.T., Kim, M.C., Choi, J. and Heo, N.H. 2000. Molten-salt method for the synthesis of zeolitic materials: I. Zeolite formation in alkaline molten-salt system. *Microporous and Mesoporous Materials* 37(1–2), pp. 81–89.
- Pekov et al. 2011. – Pekov, I.V., Olysysh, L.V., Chukanov, N.V., Zubkova, N.V., Pushcharovsky, D.Y., Van, K.V., Giesster, G. and Tillmanns, E. 2011. Crystal chemistry of cancrinite-group minerals with an AB-type framework: A review and new data. I. Chemical and structural variations. *The Canadian Mineralogist* 49, pp. 1129–1150.
- Tanaka, H. and Fujii, A. 2009. Effect of stirring on the dissolution of coal fly ash and synthesis of pure-form Na-A and -X zeolites by two-step process. *Advanced Powder Technology* 20(5), pp. 473–479.
- Querol et al. 2001 – Querol, X., Umana, J.C., Plana, F., Alastuey, A., Lopez-Soler, A., Medinaceli, A., Valero, A., Domingo, M.J. and Garcia-Rojo, E. 2001. Synthesis of zeolites from fly ash at pilot plant scale. Examples of potential applications. *Fuel* 80(6), pp. 857–865.
- Querol et al. 2002 – Querol, X., Moreno, N., Umana, J.C., Alastuey, A., Hernandez, E., Lopez-Soler, A. and Plana, F. 2002. Synthesis of zeolites from coal fly ash: an overview. *International Journal of Coal Geology* 50, pp. 413–423.
- Wdowin et al. 2014 – Wdowin, M., Franus, M., Panek, R., Badura, L. and Franus, W. 2014. The conversion technology of fly ash into zeolites. *Clean Technologies and Environmental Policy* 16, pp. 1217–1223.
- Zhang et al. 2017 – Zhang, Z., Xiao, Y., Wang, B., Sun, Q. and Liu, H. 2017. Waste is a misplayed resource: Synthesis of zeolites from fly ash for CO₂ capture. *Energy Procedia* 114, pp. 2537–2544.
- Zhao et al. 1997 – Zhao, X.S., Lu, G.Q. and Zhu, H.Y. 1997. Effects of Ageing and Seeding on the Formation of Zeolite Y from Coal Fly Ash. *Journal of Porous Materials* 4, pp. 245–251.

SYNTHESIS OF PITIGLIANOIT AND TOBERMORITE FROM FLY ASH ORIGINATING FROM LIGNITE COMBUSTION

Keywords

fly ash, tobermorite, pitiglianoite, melilite

Abstract

Fly ash which has been separated from the flue gas stream as a result of fossil fuels combustion constitutes a huge amount of waste generated worldwide. Due to environmental problems, many directions of their rational use have been developed. Various attempts to convert fly ash into sorption materials, mainly synthetic zeolites, are conducted successfully. In this paper, an attempt was made to convert fly ash from lignite combustion from one of the Polish power plants, using alkaline hydrothermal synthesis. The primary phases in the fly ash were: quartz, gehlenite, mullite, hematite, feldspar, lime, anhydrite, occasionally grains of ZnO phase and pyrrhotite, glass and unburned fuel grains. As a result of hydrothermal synthesis a material containing new phases – pitiglianoite and tobermorite was obtained. Among the primary ash constituents, only gehlenite with an unburned organic substance, on which tobermorite with crystallized pitiglianoite was present. As a result of detailed testing of products after synthesis, it was found that among the tested grains:

- two populations can be distinguished – grains containing MgO and Fe₂O₃ as well as grains containing Fe₂O₃ or MgO or containing none of these components,
- the main quantitative component was pitiglianoite,
- pitiglianoite was present in larger amounts in grains containing Fe₂O₃ or MgO or in the absence of both components than in grains in which Fe₂O₃ and MgO were found.

The results of the study indicate that in post-synthesis products, the contribution of components were as follows: pitiglianoite – 39.5% mas., tobermorite – 54% mas., gehlenite – 3% mas. and organic substance – 3.5% mas.

SYNTEZA PITIGLIANOITU I TOBERMORYTU Z POPIOŁU LOTNEGO POCHODZĄCEGO ZE SPALANIA WĘGLA BRUNATNEGO

Słowa kluczowe

popiół lotny, pitiglianoit, tobermoryt, melilit

Streszczenie

Popioły lotne po separacji ze strumienia gazów spalinowych, powstałych ze spalania paliw kopalnych, stanowią ogromne ilości w światowej skali odpadów. Z uwagi na problemy środowiskowe opracowano wiele kierunków ich racjonalnego wykorzystania. Z powodzeniem podejmowane są różne próby wykorzystania popiołów lotnych do materiałów sorpcyjnych, głównie syntetycznych zeolitów. W niniejszej pracy podjęto próbę wykorzystania popiołu lotnego pochodzącego ze spalania węgla brunatnego z jednej z polskich elektrowni, z zastosowaniem syntezy hydrotermalnej alkalicznej. W składzie mineralnym badanego popiołu lotnego stwierdzono obecność kwarcu, gehlenitu, mullitu, hematytu, skaleni, wapna, anhydrytu, sporadycznie ziaren fazy ZnO i pirotynu, szkliwa i ziaren nieprzepalonego paliwa. W materiale po hydrotermalnej syntezie popiołu lotnego stwierdzono obecność nowych faz – pitiglianoitu i tobermorytu. Wśród pierwotnych składników popiołu obecny był jedynie gehlenit z niespaloną substancją organiczną, na których krystalizowały nowe fazy. W wyniku szczegółowych badań produktów po syntezie stwierdzono, że wśród badanych ziaren:

- można wyróżnić dwie populacje – ziarna zawierające MgO i Fe₂O₃ oraz ziarna zawierające Fe₂O₃ lub MgO lub niezawierające żadnego z tych składników,
- głównym ilościowym składnikiem był pitiglianoit,
- pitiglianoit obecny był w większych ilościach w ziarnach zawierających Fe₂O₃ lub MgO lub przy braku obu tych składników, niż w ziarnach, w których stwierdzono obecność Fe₂O₃ i MgO.

Wyniki badań wskazują, że w produktach po syntezie udział składników był następujący: pitiglianoit – 39,5% mas., tobermoryt – 54% mas., gehlenit – 3% mas. i substancja organiczna – 3,5% mas.